

Acoustic spectra characteristics of atmospheric pressure plasma using optical wave microphone

Abstract. We apply the new method to examine electric discharge sound using Fraunhofer diffraction effect of visible laser beam. This new system is called the optical wave microphone and is very useful for the detection of sound wave without disturbing the sound field. Applied voltage, current and the electrical discharge sound of Coplanar DBD (Dielectric Barrier Discharge) are measured, and the fundamental relationship between the discharge and the acoustic properties is examined. The Fast Fourier Transform (FFT) is applied to discriminate the acoustic sound of the Coplanar DBD discharge and the dominant frequency components.

Streszczenie. Praca przedstawia nową metodę analizy dźwięku wyładowania elektrycznego przy użyciu efektu dyfrakcji Fraunhofera wiązki światła laserowego w widzialnym zakresie widma. Zaproponowane rozwiązanie zostało nazwane mikrofonem optycznym. Jest ono szczególnie korzystne przy detekcji fali dźwiękowej gdyż nie dochodzi wtedy do zaburzeń pola dźwiękowego. Zmierzono prąd, napięcie i dźwięk podczas barierowego wyładowania elektrycznego i dokonano analizy podstawowych zależności między parametrami wyładowania i właściwościami akustycznymi, do których opracowania wykorzystano algorytm szybkiej transformacji Fouriera. (Widmo akustyczne plazmy o ciśnieniu atmosferycznym użyte jako mikrofon optyczny)

Keywords: electric discharge, sound signal, laser light diffraction, optical wave microphone.

Słowa kluczowe: wyładowanie elektryczne, sygnał dźwiękowy, dyfrakcja światła laserowego, mikrofon optyczny.

1. Introduction

Dielectric barrier discharges are very attractive for industrial applications because they can provide non-equilibrium plasma conditions at atmospheric pressure. Traditionally used for industrial ozone production, DBD have been focused on other practical applications such as surface treatment, pollution control (including the removal of the environmental pollutants such as NO_x, SO_x, VOCs), large area flat plasma displays, plasma actuators, etc. Further applications are expected [1,2], which may include DBD's use in greenhouse gas control technologies. The coplanar electrical discharge, where the electrode arrangements consist of two electrodes embedded inside a dielectric with a fixed electrode distance, also belongs to DBD group. The investigation of coplanar DBD phenomenon mainly examines voltage, current, and luminescence. To our best knowledge, using the electrical discharge sound has not been used for this purpose as yet. To examine the fundamental characteristics of coplanar DBD; voltage/current signals and the electrical discharge sound are measured, and the fundamental relationship between the discharge and the acoustic properties is examined. However, it's not easy to detect the sound signal in plasma reactor by the conventional condenser microphone technique [3-5]. Therefore, we developed a new diagnostic method (optical wave microphone), in which sound wave is measured by an optical sensor based on a Fraunhofer diffraction effect [6-10] between the sound wave and laser beam. The optical wave microphone is very useful to detect not only audible sound but also ultrasonic sound wave without disturbing the sound field. In addition, the optical wave microphone has a potential to diagnose the plasma state even during operation because this measurement system is totally insulated.

In this paper, we measured the ultrasonic wave emitted from the coplanar DBD using the optical wave microphone. The condenser microphone was also used for comparison. The time-resolved waveforms of the applied voltage, the current and the ultrasonic wave were measured simultaneously and the relationships were analyzed. FFT analysis was also performed to identify the frequency components.

2. Experimental procedures

2.1 Principles

The fundamental optical setup of the Fraunhofer diffraction measurement is shown in Fig1, where the laser beam is assumed to be of Gaussian type [10]. When the incident probing laser beam crosses a sound wave as shown in Fig.1, diffracted waves are generated and propagate with the penetrating beam through the Fourier optical system. Further, they reach the observing plane, which is set at the Fraunhofer diffraction region or in the back focal plane of the first receiving lens, placed one focal length beyond the Gaussian beam waist. The diffracted optical waves are homodyne-detected there by using the penetrating optical wave as a local oscillating power. The intensity of diffracted waves of higher orders is much smaller than that of the first order wave and can be neglected. The spatial intensity (I_{ac}) of the resultant optical field at the back focal plane is given by the equation (1) [3-4,11]. We are calling this setup an optical wave microphone.

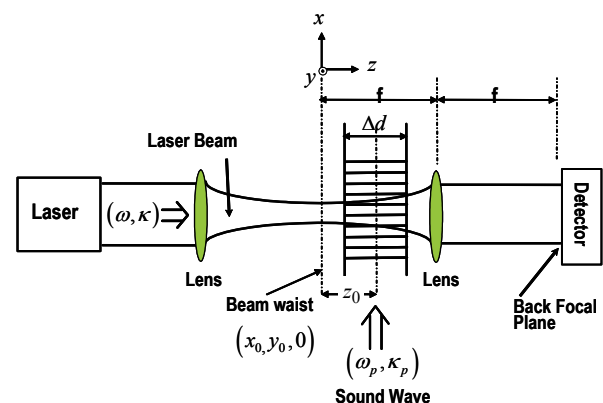


Fig.1. Schematic representation of optical wave microphone.

(1)

$$I_{ac} = I_0 \Delta \phi_0 \left[\exp\left\{-\left(u^2 + (u - \theta)^2\right)\right\} - \exp\left\{-\left(u^2 + (u + \theta)^2\right)\right\} \right] \sin \omega_p t$$

where

$$I_0 = \left(2P_0 / \pi w_f^2\right) \exp\left[-2\left(y_f / w_f\right)^2\right]$$

$u = x_f / w_f$: the normalized x -coordinate in the back focal plane, $\theta = k_p w_0 / 2$: the normalized wave number, w_f : the beam size in the focal plane, $k_p (= 2\pi / \lambda_p)$: the wave number of sound wave, w_0 : the spot size, P_0 : the total incident power, $k_i (= 2\pi / \lambda_i)$: the wave number of incident beam, λ_i : the wave length of probing beam, $\phi_0 = \kappa_i (\mu_0 - 1) \Delta d$: the time-constant of component of phase modulation, $\Delta \phi_0 = \kappa_i \Delta \mu_0 \Delta d = \kappa_i (\mu_0 - 1) \Delta d \Delta p / \gamma p$: the time-dependent component of phase modulation, μ_0 : the reflective index of air, γ : the specific heat ratio, Δd : the width of sound wave, p : the air pressure, Δp : the intensity of sound wave, $\rho = z_0 / Z_R$: the spatial position parameter of sound wave normalized by the Rayleigh zone, z_0 : the distance from the beam waist to the wave position, and $Z_R = \kappa_i w_0^2 / 2$: the Rayleigh zone.

2.2 Experimental apparatuses

The coplanar DBD is generated in order to understand the relationship between the discharge and the acoustic properties. The electrodes to generate the coplanar DBD are commonly used in ac plasma displays, which consist of two-electrodes system embedded inside a dielectric with a fixed electrode distance. This type of discharge also has been used as an ozonizer but has recently attracted much attention because of its potential as a plasma actuator.

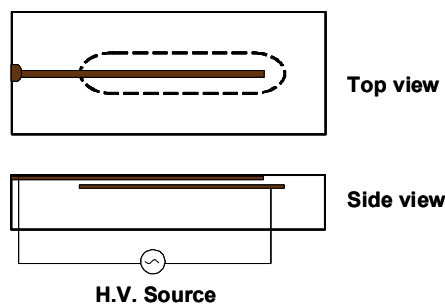


Fig.2. Top view and cross section of electrodes module.

The top view and cross-section schematic diagrams of the electrode are shown in Fig. 2. The main part of coplanar DBD was a high-purity Al_2O_3 ceramic substrate (15 mm in width, 37 mm in length, and 1.25 mm in thickness), which was also used as the dielectric. The discharge system consisted of two electrodes buried under Al_2O_3 ceramic substrate. The distance between the electrodes was 220 μm . HV electrode (1.25 mm in width, 29.5 mm in length, and 10 μm in thickness) of the surface and a grounded electrode (6 mm in width, 24.5 mm in length, and 10 μm in thickness) inside the substrate were printed by a plasma spray coating method. The discharge plasma was generated on the surface.

Figure 3 shows the experimental setup for detection of the sound signal from coplanar DBD in the air. The high voltage (6kVpp, 28.25 kHz) was produced by the high frequency and high voltage power supply. The high voltage was applied to the electrode at the atmospheric pressure. The sound signal (the audible sound wave and the ultrasonic wave) was generated by the discharge on the electrodes. The discharge current was measured through the current transformer (frequency range = 1kHz~1MHz). The applied voltage, the voltage of current transformer of coplanar discharge, and the acoustic signal were collected by the digital oscilloscope (Tektronix TDS3034). The acoustic signal was measured by the optical wave microphone and the condenser microphone (Rion, UC-29, 20 -100 kHz). The condenser microphone was set up 2 cm away from the electrode and the proving laser beam (685nm, 28mW, ϕ 2mm) of optical wave microphone passed through 1cm above the discharge device. Therefore, the distance of the optical wave microphone and the condenser microphone was 1cm. The sound wave reached the optical wave microphone after a delay of 29.4 μs from the condenser microphone (the sound speed was assumed to be 340 m/s). The discharge sound crossed the laser beam between the laser beam and Lens1. The diffracted laser beam was formed via the optical Fourier transform by the Lens1 and detected by the photodiode detector. The diameter of the laser, which reaches to the photodiode detector was adjusted by the beam expander (Lens2 and Lens3). The lowest frequency was limited by the background noise level of about 50-60 dB in the experimental room. The optical signal intensity was found to be linearly proportional to the sound pressure under the condition less than 110 dB [7, 12]. The amplitude of output signal of optical wave microphone was also linearly proportional to the sound frequency, which is consistent with the theoretical analysis prediction [12].

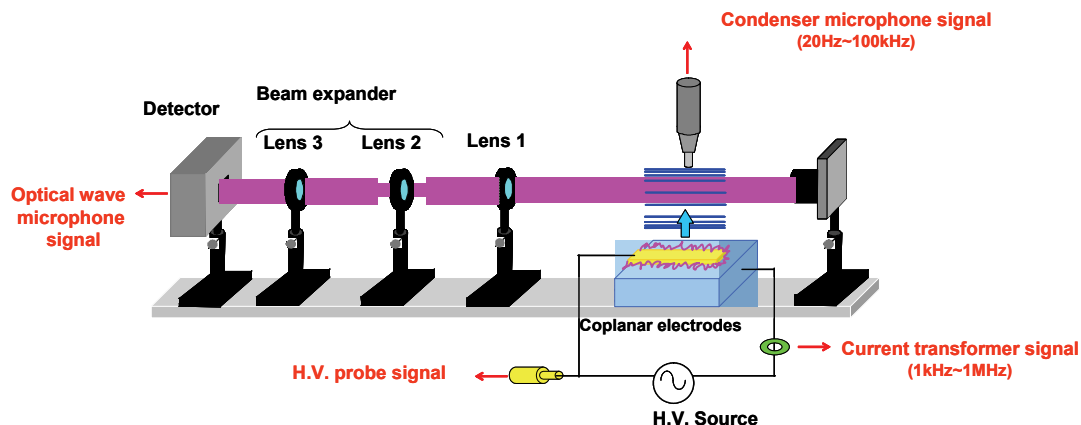


Fig.3. Experimental setup to detect the coplanar discharge sound.

The intensity of the output signal of optical wave microphone changed from 5 mV to 8 mV with the increase of sound frequency (sound pressure: 84 dB) from 25 kHz to 50 kHz. However, the output signal unit was described by voltage to stay in agreement with linear system unit. Of course, the processing of the frequency-independency of output signal is possible by the electric circuit or computer software if necessary.

3. Results and discussion

Before the measurement, the stability and the uniformity of the light emission from the discharge were confirmed. The stabilized discharge generated ozone with the generation rate of approximately 10 mg/h. Therefore, the main atmosphere around the laser beam was not only the air but also ozone. In this paper, we report a result of time-resolved optical wave microphone signal for the discharge in air; however, we confirmed that this method had a potential to detect the type of atmosphere and its pressure. Since the surface discharge is one of the non-thermal plasmas, it was assumed that the temperature of the detecting region is constant at the room temperature.

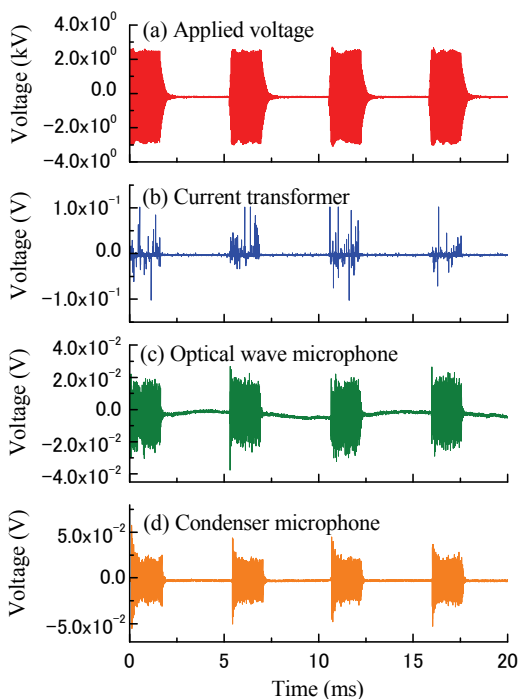


Fig.4. Typical voltage waveforms obtained from (a) High voltage probe, (b) Current transformer, (c) Optical wave microphone and (d) Condenser microphone.

Figure 4 shows the typical voltage waveforms obtained from (a) high voltage probe, (b) current transformer, (c) optical wave microphone, and (d) condenser microphone. The measurement time was 20ms and the duty ratio of voltage waveform was 0.43. When the high voltage was applied to the electrode, the discharge current appeared and the discharge sound was generated. The sound has been detected by the optical wave microphone and the condenser microphone. These generation time of the discharge current and the sound signal are in fairly good agreements. As the duty ratio increased, the electrical discharge phenomenon became more active. When the sinusoidal signal of frequency 50 kHz and sound pressure 84 dB was detected by the optical wave microphone, the output signal of microphone became 8 mV (see Section 2.2).

Therefore, if the dominant frequency component of discharge sound was 50 kHz, the sound pressure could be estimated as 92 dB because of the peak value of output voltage of the optical wave microphone was 20 mV or more.

Figure 5 shows the FFT spectra of voltage waveforms obtained from (a) high voltage probe, (b) current transformer, (c) optical wave microphone and (d) condenser microphone. The frequency range for FFT analysis is shown from 0 to 250 kHz (the sampling frequency to store in the digital oscilloscope was 500 kHz). The current was composed of the pulsed discharge current and the displacement current due to the capacitance of the device ceramics. The coplanar DBD occurred two times in a cycle of applied voltage. The FFT result for the current transformers is shown in Fig. 5(b) with the current having wide frequency components from 0 to 250 kHz. The large peak appeared at 28.3 kHz which almost corresponded to the frequency of the applied voltage due to the relatively large displacement current. Many smaller peaks, which may correspond to the pulsed discharge were observed within the wide range of the frequency. The FFT result of the optical wave microphone is shown in Fig. 5(c). It contained many frequency components such as 56.5, 84.6, 113.0, 141.3, 169.4 and 197.8 kHz. These values were almost same with 2nd, 3rd, 4th, 5th, 6th, and 7th harmonics frequency of applied voltage. The FFT result of the condenser microphone (Fig.5 (d)) shows that the main frequency components are 28.2 and 56.4 kHz. The condenser microphone was not able to detect the high frequency components that the optical wave microphone have detected, because the optical wave microphone is more sensitive compared the condenser microphone at the high frequency region.

Figure 6 shows time-resolved waveforms obtained from (a) high voltage probe, (b) current transformer, (c) optical wave microphone and (d) condenser microphone with 25 MHz of sampling frequency.

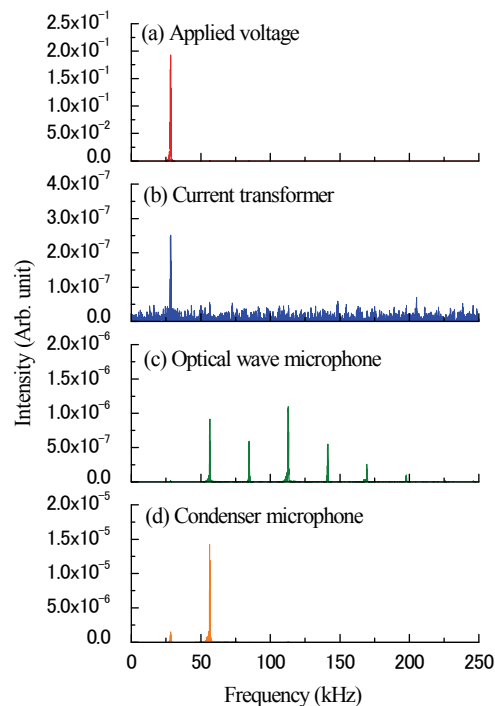


Fig.5. FFT spectra obtained from (a) High voltage probe, (b) Current transformer, (c) Optical wave microphone and (d) Condenser microphone.

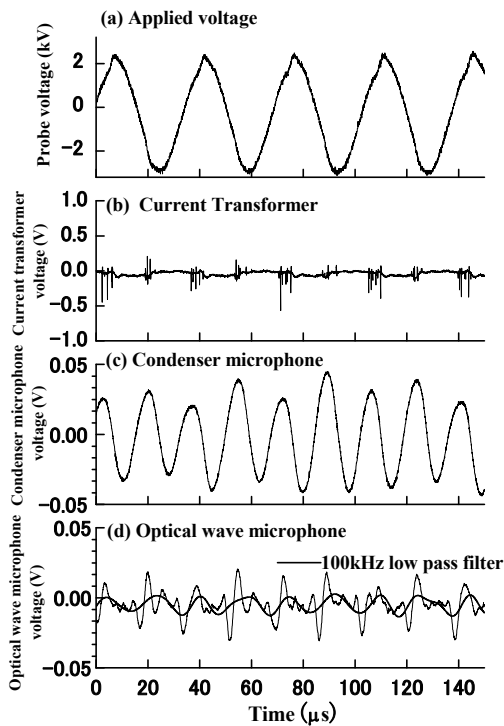


Fig.6. Time-resolved waveforms of (a) High voltage probe, (b) Current transformer, (c) Condenser microphone and (d) Optical wave microphone. The treatment of digital low pass filtering (<100 kHz) is performed for (d).

The sound signal of optical wave microphone after low-pass filter of 100 kHz is also shown at Fig.6 (c). In Fig.6(c) and (d) correction was made for the time delay from the sound emission to the detection basing on the sound velocity, the distance between the device and the condenser microphone or the laser beam of the optical wave microphone (see Section 2.2). As can be seen in

Fig.6(b), the current was composed of the pulsed discharge current and the displacement current (capacitance of the ceramics of the device was 6 pF). It was obtained from the comparison of the applied voltage and the current (Fig.6(a) and (b)). The pulsed discharge current had the pulse width of a few 100 ns and flew for about 5 μ s. At this point, the time derivative of the applied voltage exhibited almost maximum value. The discharge occurred mainly two times in one cycle of the applied voltage although there were the polarity dependencies, which are well known in many reports. It is obvious that the discharge emitted the ultrasonic wave because the result observed by the condenser microphone showed the typical waveform of compression wave (Fig.6(c)). The ultrasonic wave was generated during the pulsed discharge current flow (Fig.6(b) and (c)). The optical wave microphone could detect the ultrasonic wave from the discharge as shown in Fig.6(d). As can be seen in Fig.6(d), the waveform was rather different from that of the condenser microphone. The frequency resolution of the optical wave microphone also higher comparing to the condenser microphone data. The reason of the complex waveform of the optical wave microphone is still not understood. However, it is confirmed that the waveform after the low pass filter (< 100 kHz) treatment shows a good agreement with the waveform of the condenser microphone. In this time-resolved measurement, it was found that the ultrasonic wave was emitted from the coplanar DBD. In addition, by employing the optical wave microphone it was found that the ultrasonic wave was composed from high frequency components which may have relationship with the harmonics of the applied voltage and could not be observed by the condenser microphone.

Figure 7 shows the effect of the distance between the discharge device and laser beam of optical wave microphone (a) (1cm,0), (b) (5cm,0), (c) (1cm, 90°), (d) (5cm, 90°), (e) (10cm, 90°). Each point-of laser beam is shown by polar coordinate plane. When the laser beam passed through a point (a), 1cm away from the center of the discharge device, the sound signal was detected by the optical wave microphone and the FFT (Fig.7(a)).

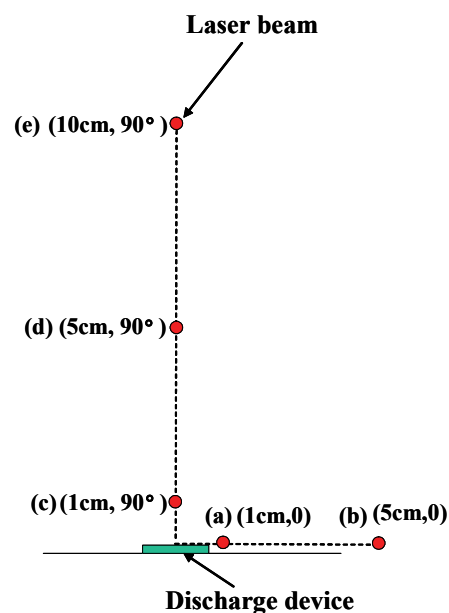
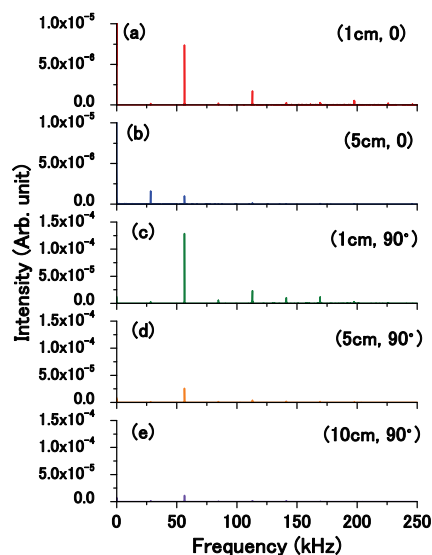


Fig.7. Effect of distance between the discharge device and laser beam of optical wave microphone (a) (1cm,0), (b) (5cm,0), (c) (1cm, 90°), (d) (5cm, 90°), (e) (10cm, 90°).

The maximum peak value was 7.39×10^{-6} at 56.45 kHz. When the laser beam horizontally moved to point (b), which was 5 cm away from the discharge device, the FFT result at 56.45 kHz decreased to 9.82×10^{-7} and this value was 13.3% of signal intensity of point (a). Moreover, the laser beam positions from the discharge device surface perpendicularly changed from 1cm to 10cm. The FFT results of discharge sound were shown in Fig. 6 (c) ~ (e) and the peak values at 56.45 kHz decreased from 1.29×10^{-4} to 2.62×10^{-5} (20.3 %) and 1.13×10^{-5} (8.76 %). The peak value of perpendicular direction 1cm away from the discharge surface (point (c)) was 1.29×10^{-4} at 56.45 kHz and this value was 17.5 times larger comparing to horizontal direction 1cm away from the center of discharge device (point (a)). These results show that the ultrasonic sound field is generated and the signal intensity of perpendicular direction of discharge surface is larger than that of horizontal one.

We consider that the optical wave microphone has a potential to give additional information for the discharge phenomenon clarification. This method can be further improved by measurements using various gases, changing gas density and investigation of the spatial relationship between the device and the laser beam.

4. Conclusion

We applied new diagnostic method of the optical wave microphone to the coplanar dielectric barrier discharge. The time-resolved waveforms of the applied voltage, the current and the ultrasonic wave were collected and the FFT analysis was performed. The obtained results are as follows:

(1) The emission of ultrasonic wave from the discharge which was synchronized with the pulsed discharge current was observed.

(2) The optical wave microphone was very useful for detection of the ultrasonic wave over 100kHz, which condenser microphone could not detect. The frequency components may have relationship with the harmonics of the applied voltage.

(3) The waveform of the optical wave microphone after the low pass filter treatment showed a good agreement with the waveform of the condenser microphone.

REFERENCES

- [1] U. Kogelschatz, B. Eliasson and W. Egli, *Pure Appl. Chem.*, 71, 1819 (1999)
- [2] J. Pons, E. Moreau, G. Touchard, *J. Phys. D*, 38, 3635 (2005)
- [3] T. Nakamiya, K. Ebihara, T. Ikegami, Y. Sonoda and R. Tsuda, *Proc. The 5th Asia-Pacific International Symposium on the Basic and Application of Plasma Technology*, 5 (2007), p.82
- [4] T. Nakamiya, K. Ebihara, T. Ikegami, Y. Sonoda and R. Tsuda, *Journal of Physics:Conf.*, 100, 062016 (2008)
- [5] T. Nakamiya, T. Tanaka, K. Ebihara, T. Ikegami. and R. Tsuda, *The Papers of Technical Meeting on Plasma Science and Technology, IEE Japan, PST-04-80* (2004), p.45
- [6] D.E. Evans, M.von Hellermann and E.Holzhauser, *Plasma Phys. Control Fusion*, 24, 819 (1982)
- [7] Y.Sonoda, Y.Suetsugu, K.Muraoka and M.Akazaki, *Plasma Phys. Control Fusion*, 25, 1113 (1983)
- [8] Y. Sonoda and M.Akazaki: *Jpn.J.Appl. Phys.* 33, 3110 (1994)
- [9] M.von Hellermann and E.Holzhauser: *IEEE Trans. Plasma Sci.* 12, 5 (1983)
- [10] T. Nakamiya, Y. Sonoda, T. Ikegami, F. Mitsugi, K. Ebihara and R.Tsuda, *PRZEGLĄD ELEKTROTECHNICZNY (Electrical Review)*, 2009, 5 (2009)
- [11] D.E. Evans, E.J.Doyle, D.Frigione, M. von Hellermann and A.Murdoch, *Plasma Phys.*, 25, 617(1983)
- [12] Y.Sonoda and Y.Nakazono, *Proceeding of 37th International Congress and Exposition on Noise Control Engineering*, No.0684,1-12 (2008)

Authors: *prof. dr Toshiyuki Nakamiya, E-mail: nakamiya@tokai.ac.jp, prof. dr Yoshito Sonoda, E-mail: ysonoda@ktmail.tokai-u.jp, prof. dr Yoichiro Iwasaki, E-mail: yiwasaki@ktmail.tokai-u.jp, Department of Electronics and Intelligent, Tokai University, Toroku9-1-1, Kumamoto 862-8652, Japan; dr Fumiaki Mitsugi, E-mail: mitsugi@cs.kumamoto-u.ac.jp, mr Shota Suyama, E-mail: s-suyama@st.cs.kumamoto-u.ac.jp, prof. dr Tomoaki Ikegami, E-mail: ikegami@cs.kumamoto-u.ac.jp, honorary prof. dr Kenji Ebihara, E-mail: k-shrimp@road.ocn.ne.jp, Graduate School of Science and Technology, Kumamoto University, Kurokami 2-39-1, Kumamoto 860-0082, Japan; prof. dr Shin-ichi Aoqui, E-mail: aoqui@cis.sojo-u.ac.jp, Department of software science, Sojo University, 4-22-1Ikeda, Kumamoto, 860-0082, Japan, prof. dr Henryka Danuta Stryczewska, E-mail: dankas@eltecopol.lublin.pl, dr Joanna Pawlat, E-mail: askmik@hotmail.com, Institute of Electrical Engineering and Electrotechnology Faculty of Electrical Engineering and Computer Science Lublin University of Technology, 38A Nadbystrzycka St., 20-618 Lublin, Poland.*